DEUTSCHES ELEKTRONEN-SYNCHROTRON DESY

DESY SR-75/09
July 1975

$N_{4,5}$ Excitations in Metallic Cesium: Single Electron Behaviour and Collective Effects

by

H. Petersen

2 HAMBURG 52 · NOTKESTIEG 1

To be sure that your preprints are promptly included in the
HIGH ENERGY PHYSICS INDEX ,
send them to the following address (if possible by air mail) :

DESY
Bibliothek
2 Hamburg 52
Notkestieg 1
Germany

$N_{4,5}$ Excitations in Metallic Cesium: Single Electron Behaviour and Collective Effects

Helmuth Petersen

Deutsches Elektronen-Synchrotron DESY

The $N_{4,5}$ excitation spectrum of Cs was measured with yield spectroscopy from the onset of transitions at 77 eV to 180 eV photon energy. Synchrotron radiation served as a light source. A broad maximum due to delayed transitions to f-symmetric continuum states is the dominating feature of the spectrum. An indication for existence of localized f-symmetric final states is found. Above the $N_{4,5}$ edges at 77.1±0.1 eV and 79.3±0.1 eV photon energy transitions to p-symmetric extended metal states are observed. Their qualitative agreement with APW band structure calculations is discussed. EDC's obtained with photon energies 75 eV and 111 eV are presented.

The observed asymmetric shape of the 4d photoemission maxima in the EDC's and the shape of the N_5 edge are discussed with regard to the final state interaction theory by Mahan, Nozieres and de Dominicis.

Das $N_{4,5}$ Anregungsspektrum von Cs wurde vom Einsatz der Übergänge bei 77 eV bis 180 eV Photonenenergie mit Hilfe der Photoausbeute-Spektroskopie gemessen. Synchrotronstrahlung diente als Lichtquelle. Das Spektrum wird beherrscht von einem breiten Maximum, das durch verzögerte Übergänge in f-symmetrische Kontinuumszustände entsteht. Anzeichen für die Existenz von lokalisierten f-symmetrischen Zuständen wurden gefunden. Oberhalb der $N_{4,5}$ Kanten bei 77,1±0.1 eV und 79,3±0,1 eV Photonenenergie wurden Übergänge in nicht lokalisierte p-symmetrische Metallzustände beobachtet. Die qualitative Übereinstimmung mit APW Bandstruktur-Berechnungen wird diskutiert. EDC's bei 75 eV und 111 eV Photonenenergie werden gezeigt. Die beobachtete Asymmetrie der 4d Photoemissionsmaxima in den EDC's und die Form der N_5 Kante werden im Hinblick auf die Theorie der Wechselwirkung der Endzustände von Mahan, Nozieres und de Dominicis diskutiert.

1. Introduction

It is well known, that in the rare earth and in La transitions into bound 4f states dominate the absorption spectra of the 4d electrons (1 to 6). This is due to the fact that the 4f states in these elements are localized within the centrifugal well of the effective potential. In Xe, on the contrary, only f-symmetric continuum states can be occupied by excited 4d electrons, transitions into bound f-states are not observed (7-9). The shift of the 4f wavefunction into the region within the potential barrier of the centrifugal well must occur somewhere in the series of the elements Xe, Cs, Ba, La. The investigation of this effects is of considerable experimental and theoretical interest.

The recently reported experimental results on atomic (10,11) and metallic (11) Ba showed only transitions to bound 4f states (12). The spectrum of metallic Ba is very similar to that of La, no metal edge is observed. The appearance of transitions into final states of p-symmetry in the spectrum of Cs vapour (13) raised the question if a metal edge was observable in the spectrum of metallic Cs and to which extent localized f-states and extended metal states would contribute to the spectrum. The observation of such transitions from the 4d shell into band states as reported in this paper offers for the first time the possibility to compare these transitions with band structure calculations. The influence of collective atomic effects (14,15) involved in the 4d photoabsorption process of metallic Cs can be estimated. Moreover, the shape of the $N_{4,5}$ edges can be discussed along the lines of the many body final state interaction theory brought forth by Mahan and others (16,17) (MND-theory).

In addition electron energy distribution curves (EDC) have been obtained at 75 eV and 111 eV photon energy. The line shapes of the 4d photoemission maxima have been analyzed in terms of the MND theory (16-18).

2. Experimental Procedure

The spectrally continuous radiation from the Deutsches Elektronen-Synchrotron DESY [19] and a special monochromator with a fixed exit beam [20] served as a light source. The photoemission of Cs was measured using an electrostatic electron energy analyzer and a channeltron multiplier. This technique offered the opportunity to measure both EDC's and yield spectra. EDC's were measured by scanning the potential of the sample relative to the entrance slit of the analyzer. A low transmission energy of the analyzer was chosen (25 eV or 50 eV) resulting in a total resolution $\geq$0.6 eV (monochromator resolution $\sim E_{phot}/500$). The photoelectric yield is known to be proportional to the absorption coefficient in the vacuum ultraviolet [21]. Yield spectra were measured at a constant retarding potential and with low resolution of the electron energy analyzer (transmission energies 100 eV to 400 eV). This improved the counting rate but did not disturb the yield measurements since only the inelastically scattered electrons are measured which are taken as being representative of the yield. Scans of the yield spectrum were made at several values of the retarding potential to permit removal of the structures due to the unscattered electrons emitted from the Cs 4d core levels.

Since an energy dependent though smooth factor is connecting yield and absorption coefficient and since in addition the photon intensity could not be measured directly, the spectrum has been corrected by multiplying with a smooth, structureless empirical function. This function was deduced from comparison of the absorption coefficient of Al [23] and the Al yield spectrum measured with the same experimental set up [22] and under virtually the same conditions concerning the spectral distribution of the light source. This deduction appears reasonable since the above mentioned smooth factor results from inelastic scattering of the excited electrons and since the $L_{2,3}$ spectrum of Al and the $N_{4,5}$ spectrum of Cs cover almost the same energy

range. The thus corrected yield curves as shown below ought to be a good approximation to the absorption coefficient of Cs. This absorption coefficient has not yet been measured directly, probably due to the difficulties encountered in preparation of thin films for absorption measurements because of the extreme chemical reactivity of Cs.

Samples were obtained sealed under vacuum in glass ampules, the quoted purities were 99.98 % (E. Merck AG., Darmstadt). An ampule (5 g) was placed in the vacuum chamber and broken open after the usual pumpdown and bakeout procedure when pressure was in the 10^{-9} range. Cs was than slightly warmed (MP 301.7 K) and poured into a boat made of tantalum. During this procedure the pressure rose to the upper 10^{-8} range due to the high vapour pressure of Cs but no effects of Cs layers on the sensitive parts of the apparatus could be observed owing to a nearly complete shielding of the analyzer by metal. The only indication of Cs vapour was a too large signal from the ionization gauge when it had not been baked out immediately before. Measurements were done on five days running at pressures in the upper 10^{-9} torr range. During this time no indications of oxid showed up on the surface of the sample or in the measured spectra. Obviously a metal rich surface was maintained for this period. This might be either due to the fact that the surface remains metallic during oxidation as reported by Helms and Spicer (24) for Sr or to a continuous evaporation of Cs from the surface. The vacuum chamber was finally vented with air and quick oxidation of the sample indicated by a gray surface took place. Spectra obtained shortly thereafter showed strong deviations from the Cs spectrum. Considerable absorption below the Cs 4d threshold in agreement with the strong absorption of oxygen in that energy region (25) was found. Sample temperatures could be varied between RT and LNT. Structures in the yield spectra obtained at LNT are more pronounced and only these spectra are shown below.

3. Experimental Results and Discussion

(A) Yield Measurements

Figure 1 shows the yield spectrum of Cs from the onset of $N_{4,5}$ transitions to 180 eV photon energy. Although the scale is arbitrary the genuine zero point is shown. Transitions to f-symmetric continuum states give rise to the strong absorption maximum dominating the spectrum. These transitions are almost completely supressed at threshold and the oscillator strength is shifted to higher energies by a potential barrier effect [9]. This feature of the spectrum is very similar to the 4d absorption spectrum of Xe [7,8] and Cs vapour [13]. Good agreement between experimental and calculated results is achieved using the random phase approximation with exchange (RPAE) [14,15,26]. Results for the Cs 4d absorption reported by Amusia are included in Fig. 1 together with absorption cross sections of outer subshells in that energy region [14]. The onset of the theoretical curve (4d absorption). The threshold of calculated 4d→Ef transitions occurs at a higher energy than in the experiment because atomic relaxation effects are not included in the RPAE.

Structure around 95 eV is very similar to that observed in the Cs-halides [27]. It was interpreted as a double excitation of a 4d and a 5p electron of Cs. These double excitations were observed with a similar shape in CsCl vapour [28], and also far less pronounced and of window type line character, in atomic Cs. This indicates that a second effect observable only in solids and molecular gases but not in monoatomic vapours is involved. Structure at 95 eV might therefore be partly due to scattering of the outgoing electron wave function from the neighbouring atoms back to the excited atom. Positive or negative interference modulates the matrix element, thus generating the minima as a function of the electron wavelength [29 to 32]. This extended X-ray absorption fine structure (EXAFS) mechanism has been verified for the extended

structure in the $L_{2,3}$ absorption spectra of Na and Al [22,33]. The weak minimum at about 108 eV can probably be explained in the same way. The small peak at 160 eV is due to the onset of transitions from the $4p_{3/2}$ level of Cs. Its low intensity precludes a more extensive analysis.

Figure 2 gives the spectrum near the $N_{4,5}$ threshold in an enlarged scale together with the spectra of Cs vapour and Cs oxid. A structure similar to that called D and F_d^+ was observed in all solid Cs halides (F_d^+) [27] and in CsCl vapour [28] at a photon energy of about 85 eV. These structures in the Cs-halides have not yet been assigned. The insensitivity of structure around 85 eV to the local environment of the Cs ion supports an interpretation as a transition to a strongly localized f-symmetric final state bound in the Cs core within the potential barrier. Such an interpretation is confirmed by our Hartree Fock calculations for atomic Cs performed using a program developed by Froese-Fischer [34], which indicated a reasonable though small oscillator strength for transitions to bound 4f states. The structures at 85 eV are therefore assigned to a transition $4d^{10}5s^25p^6\ {}^1S_o \rightarrow 4d^94f^15s^25p^6$. A term value ($^1P_1$, $^3P_1$, or $^3D_1$) of the final state configuration could not be determined. Structure around 85 eV in the absorption coefficient of Cs vapour can probably be interpreted in the same way. Its different appearance is presumably caused by multiplett splitting due to interaction with the 6s electron of atomic Cs. Such an effect was found in the metal and vapour spectra of Ba too [11]. A spin-orbit mate of structure D with an energetic distance of about 2.2 eV is not observed and could not be found unambiguously in the spectra of the Cs halides. This might be caused by strong coupling between the 4d hole and the 4f electron because of which the LS-coupling scheme rather than the jj-coupling scheme has to be applied.

Figure 3 shows the structure A,B,C at the onset of transitions after subtraction of the background indicated in Fig. 2. Included is a density of states (DOS)

calculation for the p-symmetric part of the conduction band performed by Kmetko [35] using a program developed by Wood (APW-method) [36]. The spin-orbit splitting was obtained from the EDC measurements reported below. The spin-orbit pairs have been weightened 3:2 according to the relative degeneracy of the two core levels. Although a possible slight variation of the matrix element in the energy range shown in Fig. 3 is not taken into consideration, the agreement between theory and experiment is good. The different shapes of A and B as well as the peak C are reproduced. The excitations to the p-symmetric states are obviously single electron like. Wendin's statement that in atoms the excitation is not collective for $\ell \rightarrow \ell-1$ transitions [15] holds for solid Cs too as Fig. 3 demonstrates.

As can be deduced from comparison of the Cs metal and vapour spectra in Fig. 2 the separation between the two maxima in the DOS is the same as that between transitions to 6p and 7p final states in the atom (structures 1', 2', 3' and 5' respectively for the $4d_{3/2}$ core level). This reflects the atomic origin of these features of the band structure calculation. The absolute energy of transitions is shifted by 1.4 eV to lower energies in the metal.

The Cs N_5 absorption edge is obviously represented by the steep increase at the onset and ends at the small bend where DOS structure begins to determine the shape of the curve. Using the Al_3 edge (72.72 eV) for calibration its position (50 % value) was determined to be 77.1±0.1 eV. Figure 4 shows the N_5 edge to which our edge shape analysis is restricted because of DOS structure underlying the N_4 edge (79.3±0.1 eV). Included is a linear approximation of the DOS beginning at the Fermi step. The ascent value was derived from the theoretically determined DOS with the almost linear increase of the experimental curve above the edge taken into account. The width of the Fermi step at LNT (6.6 meV) is neglected. A very good fit to experiment (dashed line) is obtained by con-

volution of the DOS with a Gaussian distribution

$$f(E) = \left((2\pi)^{1/2}\Gamma\right)^{-1} \exp -E^2/2\Gamma^2 \qquad (1)$$

with Γ = 0.078 eV corresponding to 0.18 eV FWHM. This value is in excellent agreement with that obtained from a quadratic superposition of the resolution function of the monochromator (FWHM ~0.15 eV at 77 eV) and a theoretically determined 4d core level width of 0.1 eV FWHM.

The 0.1 eV core level width was calculated by McGuire [37] from theoretical atomic Auger rates. The Auger decay mechanism of the Cs 4d core hole was experimentally verified in the EDC measurement reported below. The value 0.10 eV is in agreement with a 4d core level width of 0.10 eV estimated from the atomic Cs absorption measurements. A similar value (0.09 eV) was reported by Ederer and Manalis [38] for the Xe $4d_{5/2}$ level. Broadening and rounding of the absorption edge due to the many body effect described by Mahan, Nozieres and de Dominicis has not to be invoked to explain its shape and a possible contribution to the edge width due to this effect must have a value far less than 0.1 eV. The curve labeled MND in Fig. 4 will be discussed below.

(B) Energy Distribution Curves

Figure 5 shows EDC's of Cs excited by photons of 75 eV and 111 eV energy. Resolution is about 0.9 eV. With $h\omega$=75.1 eV (upper curve) the 4d electrons are not excited. The energetic position of the $4d_{5/2}$ level relative to the Fermi level has been deduced from the yield measurements since counting rates of electrons from the valence band were extremely low. The signal was about four times as high as the dark count rate (1 count/30 sec) at 75 eV photon energy and even lower at 111 eV. Therefore the curve drawn from E_F to the $5p_{3/2}$ peak

has no quantitative significance but only indicates the observation of a signal. The low yield is due to a very small absorption cross section of the valence band for photon energies higher than the plasmon energy (39) and the rate of electrons reaching the surface without inelastic scattering is also low. Photoemission experiments on Cs by Oswald and Calcott (40) using photon energies 12 eV to 22 eV did not even show any yield from the conduction band.

As Fig. 5 shows the interpretation given in Table 1 is facilitated and strongly confirmed by comparison of EDC's with and without excitation of 4d electrons, additional structure in the 111 eV curve can be attributed without doubt to the excitation of the 4d subshell. Features due to excitation of the 5s subshell are not observed. This is similar to results from Cs-suboxides (41) and presumably partly caused by the comparatively small absorption cross section of this subshell. Its theoretical values are approximately the same as those given in Fig. 1 for outer subshells. As a consequence of the high 4d absorption cross section at 111 eV photon energy about ten times as many low energy electrons (0 eV $\leq E_{kin} \leq$ 10 eV) are produced by these photons as by 75 eV photons. This can be derived from the areas below the curves of Fig. 5.

Table 1 shows discrepancies between the observed high energy edges of the $O_{2,3}$ VV and $N_{4,5}O_{2,3}O_{2,3}$ Auger channels and the values deduced from the core level energies as measured in this experiment. According to Oswald and Calcott (40) in the case of the $O_{2,3}$ VV channel the deviation is caused by Coster-Kronig decay of the deeper $5p_{1/2}$ level. Therefore this channel should be labelled O_3 VV instead. This interpretation is in agreement with EDC's from Cs-suboxides (41) which show a $5p_{1/2}$ level much broader than the

$5p_{3/2}$ level due to the rapid Coster-Kronig decay of the $5p_{1/2}$ core hole. The real high energy edge of the $N_{4,5}O_{2,3}O_{2,3}$ channel might not be observable because it is superimposed onto inelastically scattered electrons from both the $N_{4,5}O_{2,3}$ V Auger channel and 5s,p core level excitations. The $N_{4,5}O_{2,3}O_{2,3}$ Auger transitions observed at a kinetic energy around 45 eV predominantly determine the width of the Cs 4d levels. This can be seen from comparing intensity to the other observed Auger decay channel $N_{4,5}O_{2,3}$ V. Concerning the level width radiative decay is not of importance as the ratio of the total radiative decay to the total decay rate is $\sim 8.9\times10^{-5}$ (37).

Figure 6 shows the region of the 4d levels in an enlarged scale and at a better resolution (0.6 eV) after subtraction of the scattered electron background. The characteristic energy loss (CEL) structure at 79.5 eV is due to creation of a surface plasmon. The energy difference of 2.1 eV between the $4d_{3/2}$ level and the energy loss structure is in agreement with data from Kunz (42) and from Oswald and Calcott (40). The plasmon belonging to the $4d_{5/2}$ peak is not observed since it coincides with the $4d_{3/2}$ level. The shape of the 4d levels displays a considerable asymmetry. Doniach and Sunjic (18) ascribed this effect to the coupling of the core hole to the Fermi sea of conduction electrons as a consequence of the MND many body theory. Their line shape function is (18,43)

$$Y(E) = \frac{\cos\left(\pi\alpha/2+(1-\alpha)\ \arctan\ E/\gamma\right)}{(E^2+\gamma^2)^{(1-\alpha)/2}} \qquad (2)$$

Here γ is the lifetime width of the core level and α is an asymmetry parameter, which is related to the partial wave phase shifts δ_ℓ:

$$\alpha = 2\cdot \sum_{\ell=0}^{\ell max} (2\ell+1)(\delta_\ell/\pi)^2 \qquad (3)$$

The best fit (Fig. 6) was obtained with $\alpha = 0.20$, $\gamma = 0.26$ eV. The fit to the $4d_{3/2}$ peak is poor because of the underlying plasmon energy loss structure. The asymmetry parameter α should not be influenced by the resolution function of the monochromator and the electron energy analyzer, since both are symmetric to a good approximation. The parameter γ does of course not represent the lifetime width of the 4d core hole, but it includes contributions from both resolution functions.

The MND threshold exponents α_ℓ are related to α according to

$$\alpha_\ell = \frac{2\delta_\ell}{\pi} - \alpha \qquad (4)$$

Therefore the influence of the MND many body effect on the N_5 edge shape should be determined by the observed asymmetry of the $4d_{5/2}$ photoemission peak. In equ. (4) the Doniach-Sunjic asymmetry parameter α is better known as the "orthogonality catastrophe" contribution (44). This contribution tends to make the exponents negative, thus causing the threshold absorption to vanish and giving rise to an asymmetric edge shape.

To determine δ_1 and thus α_1 which is the relevant MND threshold exponent for transitions to p-symmetric final states (ℓ=1), a three-phase-shift analysis ($\ell_{max} = 2$ in equ. (3)) is appropriate because of the high d-symmetric DOS at the Fermi level (35,43). The choice of the ratio $\frac{\delta_2}{\delta_1}$ used as a parameter in Ref. 43 does only slightly influence δ_1. Its value is about 0.13 assuming a ratio $\frac{\delta_2}{\delta_1} = 0.4$, which seems to be reasonable with regard to the DOS at the Fermi level. The partial wave phase shift $\delta_1 \sim 0.13$ corresponds to an MND threshold exponent $\alpha_1 \sim -0.12$ (equ. (4), $\alpha = 0.20$).

According to the MND theory this exponent gives rise to a modification of the transition intensity I_ℓ to p-symmetric final states [16,17]:

$$I_\ell(E) \sim I_\ell^o(E)\ (\varepsilon_o/E-E_F)^{\alpha_\ell}\ , \quad \ell = 1 \qquad (5)$$

Here E is the conduction state energy, E_F the Fermi energy which is 1.8 eV in Cs [46] and I_o is constant near the Fermi level and of the order of the Fermi energy. $I_\ell^o(E)$ is the one-electron transition intensity to p-symmetric final states which is virtually proportional to the p-symmetric DOS (DOS_1) since a possible small variation of the matrix element in the energy range $E_F \leq E \leq E_F + 0.3$ eV discussed here can be neglected. Therefore

$$I_1(E) \sim DOS_1(\varepsilon_o/E-E_F)^{\alpha_1} \qquad \varepsilon_o = 1.8 \text{ eV}, \qquad \alpha_1 = -0.12 \qquad (6)$$

with the DOS indicated in Fig. 4 should be a good approximation to the transition intensity. This quantity convoluted with the above mentioned Gaussian distribution function (Γ= 0.078 eV) is given in Fig. 4 (curve "MND,α_1=-0.12").

The modification of the DOS according to equ. (6) with the negative exponent α_1 leads to an additional contribution to the edge width of about 50 meV and to an asymmetric edge shape. This asymmetry is not observed, like in other simple metals [44] there is no evidence for the orthogonality catastrophe. Moreover, agreement with experiment concerning the edge width can only be reestablished using a physically unjustified small value of Γ($\sim$0.058 eV). On the other side, however, the N_5 edge shape can be explained within the framework of one-electron theory as shown above. It is therefore concluded that photoemission line shape asymmetries and the related edge shapes cannot be both consistently described by the MND many body theory in its present form. The inconsistency can probably be resolved when the speed at which the outgoing photoelectron leaves the region of the core hole is taken into

account. This was done in a very recent theoretical paper by Gadzuk and Sunjic (45) and led to a symmetric shape of photoemission peaks in metals when the electrons are excited by photons of an energy that equals the photoionization threshold energy.

4. Summary

Different from Ba, La and the rare earths the $N_{4,5}$ excitation spectrum of metallic Cs shows metal edges at the onset. The $N_{4,5}$ edges are observed at 77.1 eV ± 0.1 and 79.3 eV ± 0.1 photon energy. The width of the N_5 edge corresponds to a 0.10 eV wide 4d core level, which is in agreement with atomic Auger lifetime broadening calculations and with experimental results from Cs vapour. A possible contribution to the edge width due to the MND theory can be limited to values far less than 0.1 eV. Structure directly above these edges is in agreement with calculations of the p-symmetric density of states. No influence of the many electron character of 4d photoabsorption on transitions to the extended p-symmetric metal states can be observed.

At a photon energy of 85 eV Cs exhibits an indication for transitions to f-symmetric final states localized within the potential barrier of the centrifugal well. Transitions to f-symmetric continuum states are observed in the energy range 80 eV to 160 eV photon energy and, as with Xe, give rise to a broad absorption maximum dominating the spectrum. The general shape of this maximum is in fair agreement with RPAE calculations. Double excitations 4d+5p are superimposed on the maximum. Its weak structure might be partly caused by the EXAFS backscattering process.

In addition to the $5p_{3/2}$ and $4d_{3/2,5/2}$ peaks the EDC's show the Auger decay channels of the respective core holes (O_3VV, $N_{4,5}O_{2,3}O_{2,3}$, $N_{4,5}O_{2,3}V$). The observed asymmetry of the 4d peaks and the shape of the N_5 edge cannot be both consistently described by the MND many body theory in its present form. Taking into account the photon energy dependence of photoemission line shapes in metals this inconsistency can probably be resolved.

Acknowledgement

The author is grateful to Dr. C. Kunz for many fruitful discussions and helpful suggestions. He wishes to thank Dr. B. Sonntag for a critical reading of the manuscript.

References

1. J.M. Zimkina, V.A. Fomichev, S.A. Gribovskii, and I.I. Zhukova, Fiz.Tverd. Tela 9, 1447 (1967) [Sov.Phys. Solid State 9, 1128 (1967)]
2. V.A. Fomichev, T.M. Zimkina, S.A. Gribovskii, and I.I. Zhukova, Fiz.Tverd. Tela 9, 1490 (1967) [Sov.Phys.Solid State 9, 1163 (1967)]
3. R. Haensel, P. Rabe, and B. Sonntag, Solid State Commun. 8, 1845 (1970)
4. A.F. Starace, Phys.Rev. B 5, 1773 (1972)
5. J. Sugar, Phys.Rev. B 5, 1785 (1972)
6. J.L. Dehmer and A.F. Starace, Phys.Rev. B 5, 1792 (1972)
7. D.L. Ederer, Phys.Rev.Lett. 13, 760 (1964)
8. R. Haensel, G. Keitel, P. Schreiber, and C. Kunz, Phys.Rev. 188, 1375 (1969)
9. J.W. Cooper and U. Fano, Rev.Mod.Phys. 40, 441 (1968)
10. D.L. Ederer, T.B. Lucatorto, E.B. Saloman, R.P. Madden, and J. Sugar, J.Phys. B 8, L 21 (1975)
11. P. Rabe, K. Radler, and H.W. Wolff, in: E.E. Koch, R. Haensel, C. Kunz, eds., Proc. of the IV. Int.Conf. on Vacuum Ultraviolet Radiation Physics, Hamburg 1974 (Pergamon/Vieweg, Braunschweig) p. 247
12. J.E. Hansen, A.W. Fliflet, and H.P. Kelly, J.Phys. B 8, L127 (1975)
13. H. Petersen, K. Radler, B. Sonntag, and R. Haensel, J.Phys. B 8, 31 (1975)
14. M.Ya. Amusia in: E.E. Koch, R. Haensel, C. Kunz eds., Proc. of the IV. Int. Conf. on Vacuum Ultraviolet Radiation Physics, Hamburg 1974 (Pergamon/Vieweg, Braunschweig) p. 205
15. G. Wendin in E.E. Koch, R. Haensel, C. Kunz eds., Proc. of the IV. Int. Conf. on Vacuum Ultraviolet Radiation Physics, Hamburg 1974 (Pergamon/Vieweg, Braunschweig) p. 225
16. G.D. Mahan, Phys.Rev. 153, 882 (1967) and 163, 612 (1967) and Solid State Physics 29, 75 (1974)
17. P. Nozieres and C.T. de Dominicis, Phys.Rev. 178, 1097 (1967)

18. S. Doniach and M. Sunjic, J.Phys. C 3, 285 (1970)

19. R. Haensel and C. Kunz, Z. Angew. Phys. 23, 276 (1967)

20. H. Dietrich and C. Kunz, Rev.Sci.Instr. 43, 434 (1972)

21. W. Gudat and C. Kunz, Phys.Rev.Lett. 29, 169 (1972)

22 H. Petersen and C. Kunz, Submitted to Phys.Rev.Lett.

23 R. Haensel, G. Keitel, B. Sonntag, C. Kunz, and P. Schreiber, phys.stat.sol. (a) 2, 85 (1970)

24. C.R. Helms and W.E. Spicer, Phys.Rev.Lett. 28, 565 (1972) and 32, 228 (1974)

25. L.C. Lee, R.W. Carlson, D.L. Judge, and M. Ogawa, J.Quant.Spectrosc. Radiat. Transfer 13, 1023 (1973)

26. C.D. Lin, Phys.Rev. A 9, 181 (1974)

27. M. Cardona, R. Haensel, D.W. Lynch, and B. Sonntag, Phys.Rev. B 2, 1117 (1970)

28. K. Radler, Internal Report DESY, F41-74/9 (DESY Hamburg 1974)

29. D.E. Sayers, F.W. Little and E.A. Stern in B.L. Henke, J.B. Newkirk, and G.R. Mallett, eds., Advances in X-Ray Analysis, Vol. 13 (Plenum Press, New York) p. 248

30. C.A. Ashley and S. Doniach, Phys.Rev. B 11, 1279 (1975)

31. P.A. Lee and J.B. Pendry, Phys.Rev. B 11, 2795 (1975)

32. B.M. Kincaid and P. Eisenberger, Phys.Rev.Lett. 34, 1361 (1975)

33. J.J. Ritsko, S.E. Schnatterly and P.C. Gibbons, Phys.Rev.Lett. 32, 671 (1974)

34. Ch. Froese-Fischer, Computer Phys.Comm. 1, 151 (1969)

35. E.A. Kmetko, NBS Spec. Public. 323 p. 67

36. J.H. Wood, Phys.Rev. 126, 517 (1962)

37. E.J. McGuire, Phys.Rev. A 9, 1840 (1974)

38. D.L. Ederer and M. Manalis, J.Opt.Soc.Am. 65, 634 (1975)

39. U.S. Whong, E.T. Arakawa, and T.A. Calcott, Phys.Rev.Lett. 25, 646 (1970)

40. R.G. Oswald and T.A. Calcott, Phys.Rev. B 4, 4122 (1971)

41. P. Ebbinghaus and W. Braun, private communication

42. C. Kunz, Phys.Lett. 15, 312 (1965) and Z. Physik 196, 311 (1966)

43. G.K. Wertheim and S. Hüfner, Phys.Rev.Lett. 35, 53 (1975)

44. J.D. Dow, Phys.Rev. B 9, 4165 (1974)

45. J.W. Gadzuk and M. Sunjic, Phys.Rev. B (to be published)

46. J.F. Kenney, MIT Solid State and Molecular Theory Group Quarterly Progress Report No. 66, 1967 (unpublished)

47. J.A. Bearden and A.F. Burr, Rev.Mod.Phys. 39, 125 (1967)

48. C. Moore, NBS-Circular 467, Vol. III (1952)

49. W. Lotz, J.Opt.Soc.Am. 60, 206 (1970)

50. C.K. Jørgensen, H. Berthou, Det Kongelige Danske Videnskabernes Selskab Matematik-fisiske Meddeleser 38, 15 (1972)

Table I: Structure observed in this experiment and data from other sources and modifications of Cs. The final energies of the Auger electrons have been corrected for the work function of the analyzer (3.5 eV). Column (a) gives the observed high energy edges of the Auger channels relative to the Fermi level of Cs. Column (b) gives the high and low energy edges as deduced from the observed core level energies and the Cs Fermi energy of 1.8 eV (46).

Structure	Source	Sample, Method	Energy (eV)	
Core levels			Binding energy	
$5p_{3/2}$, $5p_{1/2}$	this experiment	Cs metal, UPS	11.8±0.4	
	Oswald and Calcott (40)	Cs metal, UPS	12.3±0.2	14.2±0.2
	Bearden and Burr (47)	Cs metal, XPS	11.4±0.5	13.1±0.5
	Moore (48)	singly ionized atom, photoabsorption	13.3	15.2
$4d_{5/2}$, $4d_{3/2}$	this experiment	Cs metal, photoelectric yield	77.1±0.1	79.3±0.1
	Bearden and Burr (47)	Cs metal, XPS	76.5±0.5	78.8±0.5
	Petersen et al. (13)	Cs atom, photoabsorption ionization limits	82.9±0.4	85.1±0.4
	Lotz (49)	calculation of E_B in free atom combining X-ray data, spectroscopic data and work function	79	81
	Joergensen and Berthou (50)	Cs ion in non metallic compound, XPS	84.7	86.8
Auger transitions			Final energy (a)	(b)
$N_{4,5}O_{2,3}$ V	this experiment	Cs metal, UPS	67±1	67.5-61.6
$N_{4,5}O_{2,3}O_{2,3}$	this experiment	Cs metal, UPS	52±1	54.7-39.7
$O_{2,3}$ VV (O_3 VV)	this experiment	Cs metal, UPS	12.0±0.5	13.7-8.2
O_3 VV	Oswald and Calcott (40)	Cs metal, UPS	11.8	

Figure Captions

Fig. 1 Photoyield of Cs in the region of $N_{4,5}$ transitions measured at LNT. Included are results of an RPAE calculation by Amusia (12). The experimental curve was scaled to theory to obtain agreement at the high energy side.

Fig. 2 Photoyield of Cs and Cs oxide and photoabsorption of Cs vapour (13) at the onset of 4d excitations. The given values on the ordinate were derived by scaling the curves relatively to each other at the absorption maximum (∿105 eV).

Fig. 3 Onset of 4d transitions after subtraction of absorption due to outer-subshells and 4d→Ef transitions as indicated in Fig. 2. Included is a claculation of the p-symmetric DOS by Kmetko (35). As an additional information states/atom eV are given, values refer to the j(4d)=5/2 curve. The two DOS curves are weightened 3:2 according to the relative degeneracy of the 4d core levels. Spin-orbit splitting (2.2 eV) is derived from the EDC's.

Fig. 4 Cs N_5 edge and curves calculated by convolution of a Gaussian distribution (Γ = 0.078 eV) with a linear approximation to the p-symmetric DOS as given by Kmetko (35) (curve "single e^-") and modified according to the MND theory (curve "MND, α_1= -0.12").

Fig. 5 EDC's of Cs obtained with 75.1 eV and 111.6 eV photons. For comparison of relative counting rates the same numbers were attached to the $5p_{3/2}$ peak in both curves. The absolute counting rate in the scattered electron maximum of the 111 eV EDC was ∿5000/sec.

Fig. 6 $4d_{3/2,5/2}$ peaks and CEL structure in Cs after subtraction of scattered electron background as indicated in Fig. 5. The dashed curves are fits according to the theory of Doniach and Sunjic (18).

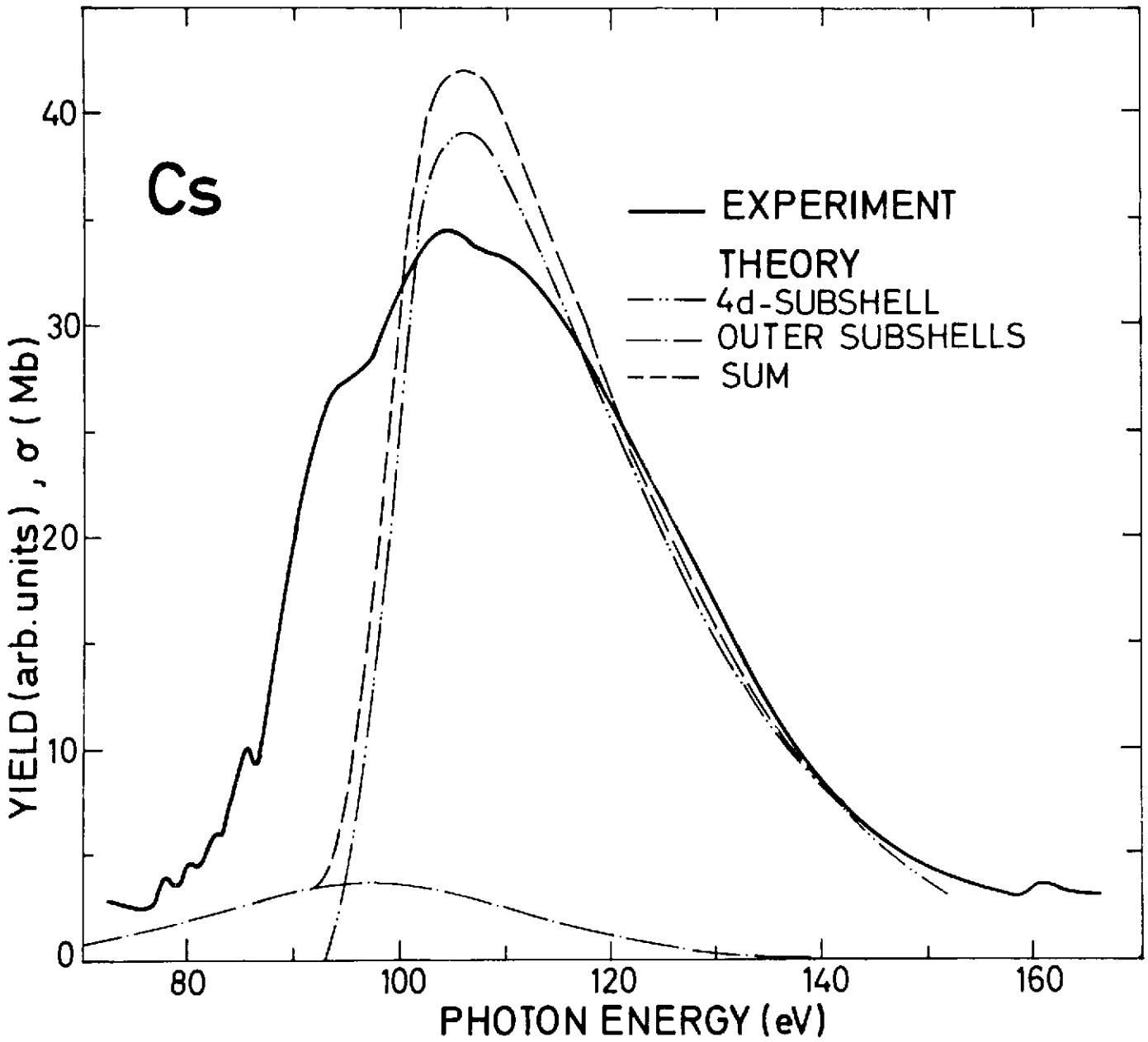
Cs
EXPERIMENT
THEORY
4d-SUBSHELL
OUTER SUBSHELLS
SUM
YIELD (arb. units) , σ (Mb)
PHOTON ENERGY (eV)
0
10
20
30
40
80
100
120
140
160

Fig. 1

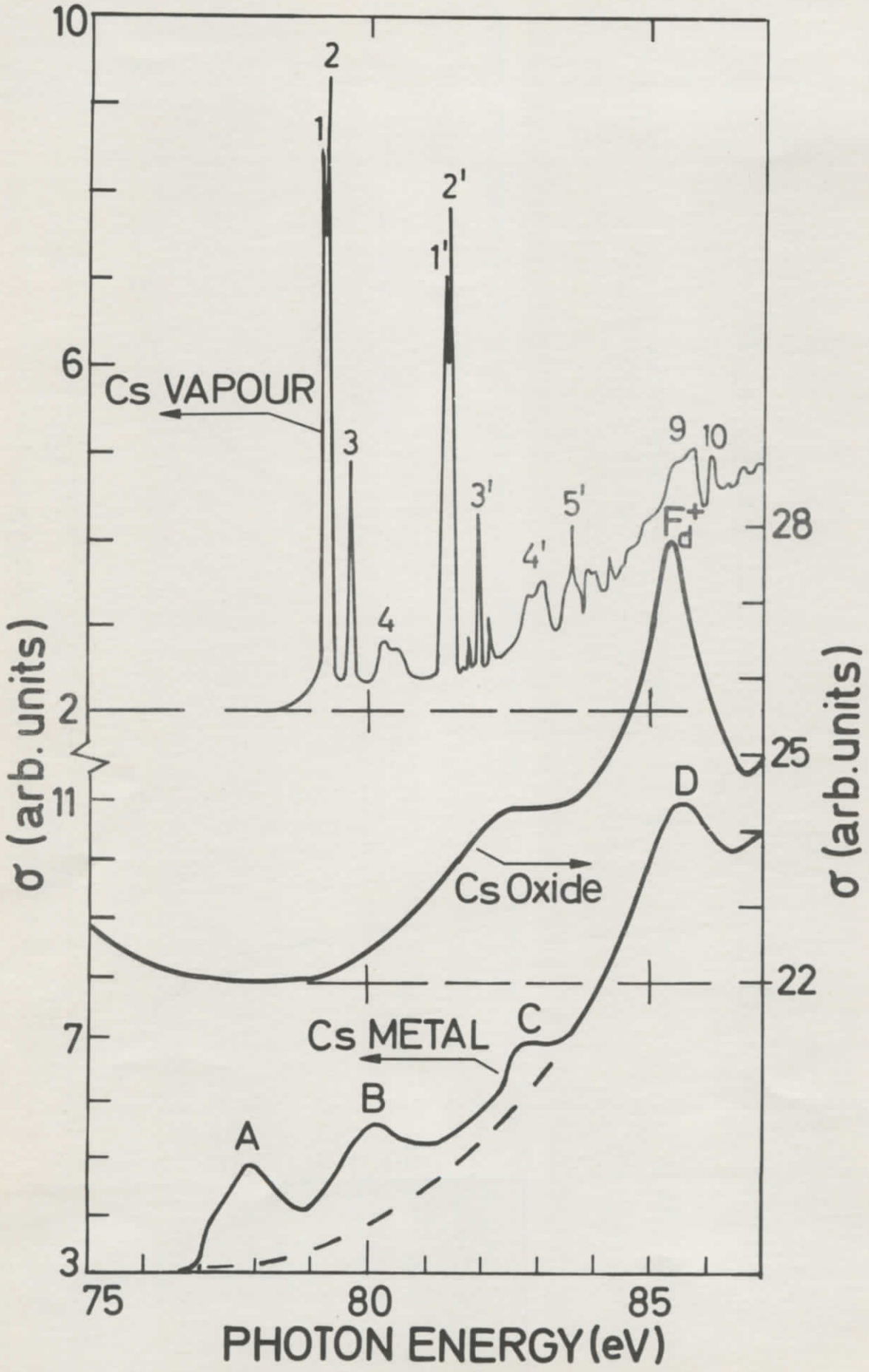
10
6
2
11
7
3
σ (arb. units)
Cs VAPOUR
1
2
3
4
1'
2'
3'
4'
5'
9
10
Fd+
28
25
22
σ (arb.units)
Cs Oxide
D
Cs METAL
C
B
A
75
80
85
PHOTON ENERGY (eV)

Fig. 2

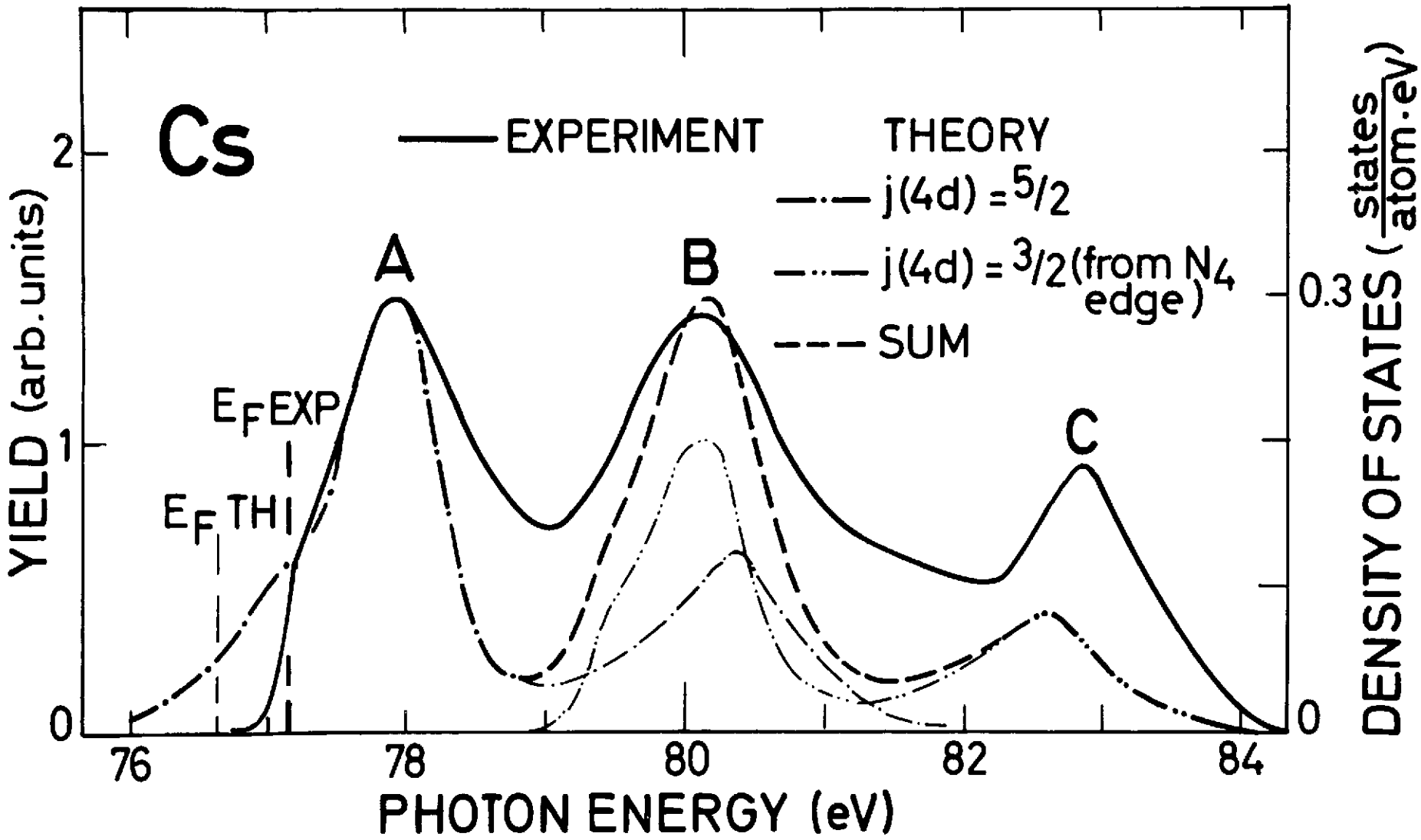
Cs
EXPERIMENT
THEORY
j(4d) = 5/2
j(4d) = 3/2 (from N4 edge)
SUM
A
B
C
E_F EXP
E_F TH
YIELD (arb. units)
DENSITY OF STATES (states / atom·eV)
PHOTON ENERGY (eV)
0
1
2
0.3
76
78
80
82
84

Fig. 3

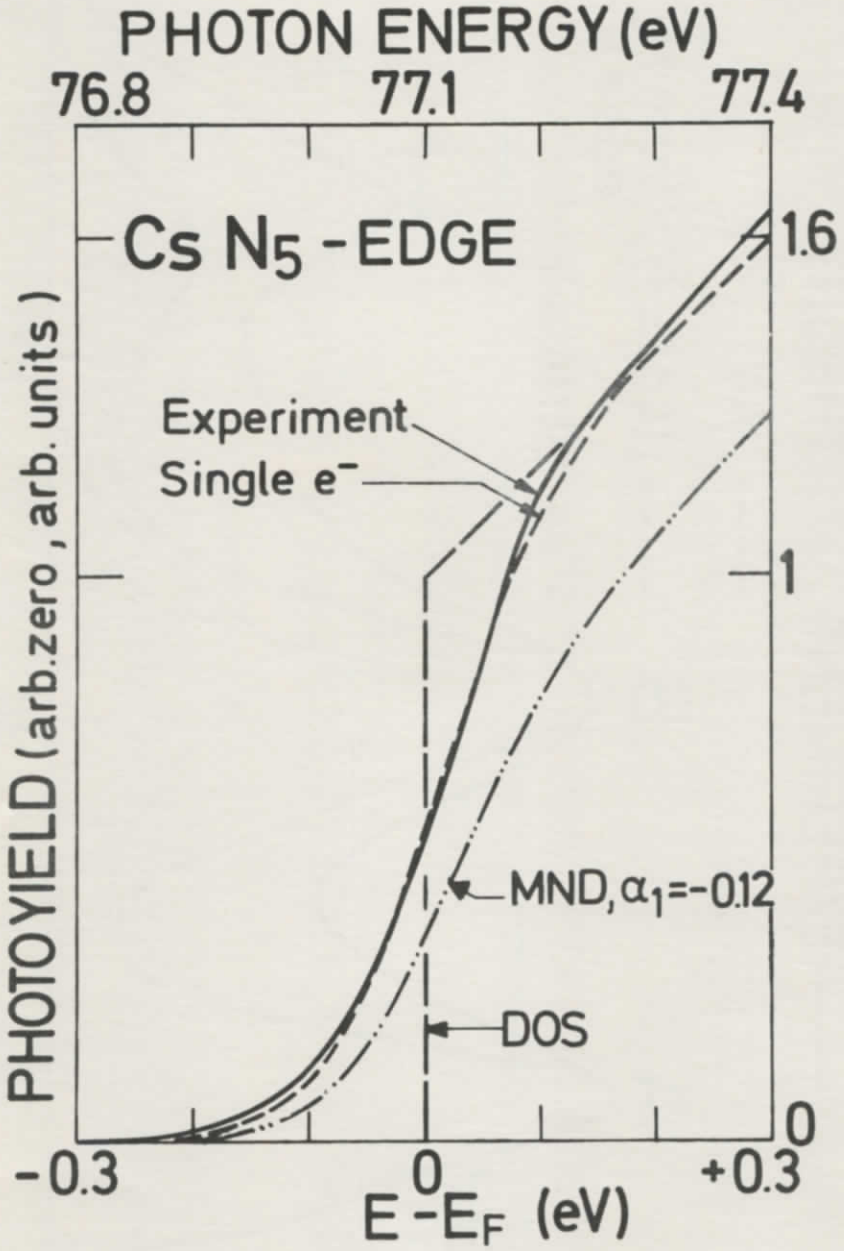
PHOTON ENERGY (eV)
76.8
77.1
77.4
Cs N5 - EDGE
1.6
1
0
Experiment
Single e⁻
MND, α1=-0.12
DOS
PHOTOYIELD (arb.zero, arb. units)
-0.3
0
+0.3
E - EF (eV)

Fig. 4

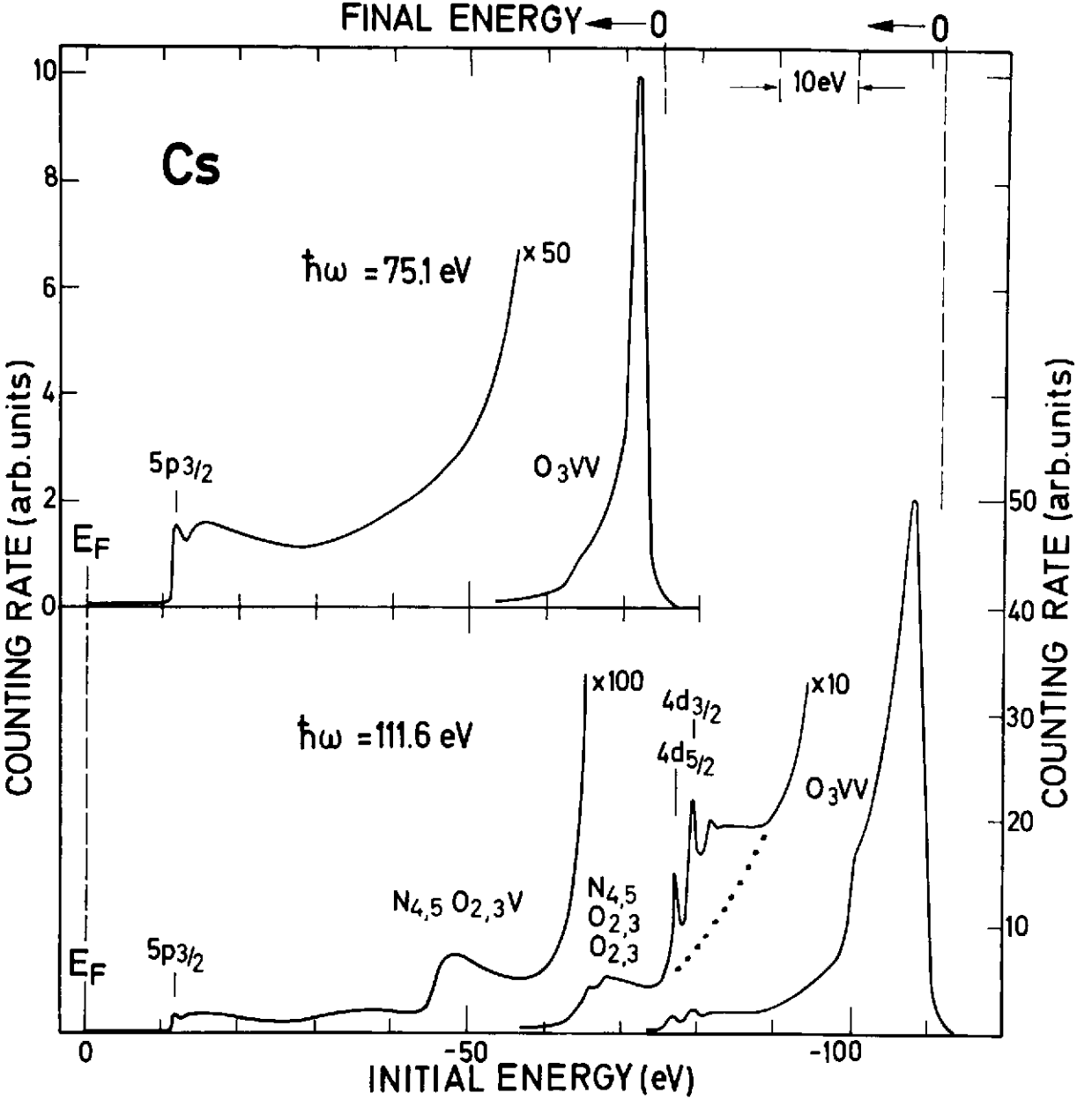
FINAL ENERGY
0
0
10eV
Cs
ħω = 75.1 eV
x 50
5p3/2
O3VV
EF
ħω = 111.6 eV
x100
x10
4d3/2
4d5/2
O3VV
N4,5 O2,3V
N4,5
O2,3
O2,3
5p3/2
EF
COUNTING RATE (arb.units)
COUNTING RATE (arb.units)
INITIAL ENERGY (eV)
0
-50
-100
10
8
6
4
2
0
50
40
30
20
10

Fig. 5

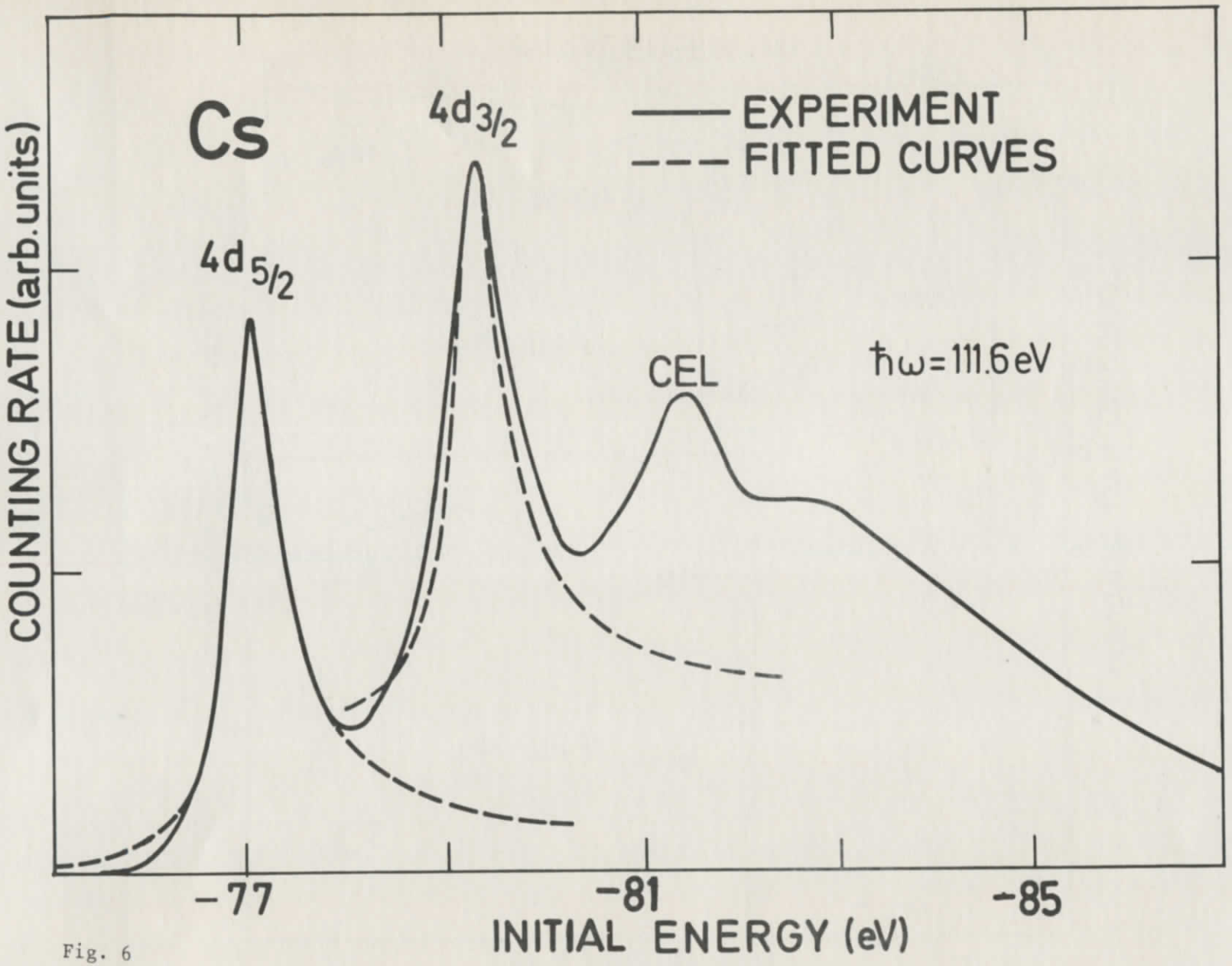
Cs
4d3/2
4d5/2
CEL
ħω=111.6eV
EXPERIMENT
FITTED CURVES
COUNTING RATE (arb.units)
-77
-81
-85
INITIAL ENERGY (eV)

Fig. 6